

# Complete models for the PN system: star, wind and nebula

S.A. Zhekov<sup>1</sup> and M. Perinotto<sup>2</sup>

<sup>1</sup> Space Research Institute, Bulgarian Academy of Sciences, Moskovska Str. 6, Sofia 1000, Bulgaria (szhekov@bgearn.acad.bg)

<sup>2</sup> Dipartimento di Astronomia e Scienza dello Spazio, Università di Firenze L.go E.Fermi 5, I-50125 Firenze, Italy (mperinotto@arcetri.astro.it)

Received 14 August 1997 / Accepted 9 January 1998

**Abstract.** We analyze the hot-bubble properties in planetary nebulae in the frame of a so called 'general' PNe picture which attempts to describe the characteristics of the planetary nebulae and their central stars in a unified manner. That is by making use of the evolutionary tracks for the central stars, the radiation driven winds theory and the interaction stellar winds model. The properties of NGC 6543 and NGC 6826 are considered in the frame of this general PNe picture. This includes specific prediction of their X-rays, EUV and infrared coronal-line radiations. In NGC 6543 we reach a satisfactory 'global' representation of the characteristics both of the nebula and of the central star, for a distance of 1.4 kpc. The calculated X-ray emission from the hot bubble of NGC 6543 agrees well with the observations by ROSAT. NGC 6826 has instead not been detected by ROSAT and future X-ray observations are needed for a better confrontation with the theory. A distance of 2.1 kpc is suitable for having a 'general' PNe picture for this object. Indication are found that the so-called super-wind is at least one order of magnitude smaller than the often quoted value of  $10^{-4} M_{\odot} \text{ yr}^{-1}$ .

**Key words:** planetary nebulae: general – planetary nebulae: individual: NGC 6543, NGC 6826 – X-rays: ISM – infrared: ISM: lines and bands

## 1. Introduction

The interacting stellar winds (ISW) model (Kwok et al., 1978; Kahn, 1983; Kwok, 1983) is nowadays widely accepted as a basic theory for the formation of the planetary nebulae (PNe). This seems to be so since: first, it is a natural consequence of the evolution of the central stars of the PNe (CSPN); second, it solves the problem with the 'sharpness' of the inner edge of the PNe, third, the ISW model is very successful in explaining the variety of shapes (symmetric as well as asymmetric) of the PNe. On the other hand, the ISW theory received much support from the observed fast winds in the central stars of PNe (CSPN), recognized to be a quite common phenomenon (e.g., Perinotto, 1993). The high velocities (600–3500 km s<sup>-1</sup>) of the CSPN winds (Patriarchi & Perinotto, 1991), are, according to

the ISW model, directly responsible for an high gas temperature in the hot bubble, which is then expected to be the source of an extended X-rays and extreme ultraviolet (EUV) radiation. The PNe should also emit infrared coronal lines (IRCL) of highly ionized species since the high temperature plasma of the hot bubble is in contact with the much colder outer shell (optical PN). As a result, the thermal conductivity is expected to play an important role for the physics of the hot bubble and an extended region of intermediate temperatures ( $5 \times 10^5 - 10^6$  K) must exist, much suited for the production of IRCL radiation (e.g., Greenhouse et al., 1993). Having this in mind, it is straightforward to conclude that a direct observational evidence for the hot bubble existence is a keypoint in the ISW model. This is why modelling of the hot-bubble characteristics and comparing them with the corresponding observables is of a great importance in order to check the validity of the model.

In this study we make use of the two-winds PN model by Zhekov & Perinotto (1996, ZhP throughout this text) in order to describe the detailed structure of the hot bubble. This is a simple 1-D model based on a similarity solution which takes into account the time-dependent characteristics of the CSPN wind as well as the effects of thermal conductivity. The latter mechanism is capable of explaining why the temperature of the X-ray emitting gas in PNe has a lower value than what is suggested by the postshock temperature corresponding to the CSPN wind velocities. Thus, the thermal conductivity effects can explain the 'softness' of the PNe X-ray spectra. For example, the observed X-ray spectra of some PNe suggest a gas temperature of a few million degrees (e.g., Kreysing et al., 1992, Arnaud et al., 1996) and the shape of the spectrum is hard to reconcile with a black-body emission corresponding to the photospheric temperature of the CSPN in these objects. On the other hand, if even a weak magnetic field is present in the PN, the effect of the thermal conductivity will be strongly suppressed in direction perpendicular to the field lines. Soker (1994) was the first who pointed out that heat conduction fronts may play an important role for the PNe physics. He also discussed the interaction of the thermal conductivity with magnetic fields. Since there is no direct evidence for the magnetic fields in PNe, it is our impression that a 'pure' conductivity model can be used to try explaining some observables of the hot bubble in PNe. Also, one of the main advantages of such a model is its simplicity in geometry since

*Send offprint requests to:* M. Perinotto

introducing of magnetic fields in the PNe physics will have as a consequence an increase of the dimensions of the problem (from 1-D to 2-D or even 3-D). Moreover, up to now the hydrodynamic simulations have paid little attention to the hot-bubble observables and this is well understood since it is technically hard to follow the PN evolution for a relatively long period of time (e.g., for a few thousand years) and also to have enough spatial (grid) resolution over the whole nebula (the optical nebula + the hot bubble). For example, Mellema & Frank (1995) have discussed the hot-bubble structure in some details but only for relatively young PNe ( $t < 1000$  years).

Another important item which should be addressed is whether the ISW model is consistent with the other theories which apply to the CSPN (e.g., the theory of stellar evolution, the radiation-driven winds model etc.), that is to have a general view of the complex object PN consisting of the nebula itself as well as of its central star. Namely, since according to the ISW model, the formation of a PN is a consequence of its central star evolution, then, the global characteristics of the PN as well as the properties of its hot bubble, being of main interest in this study, should not be arbitrarily derived by simply fitting the hot-bubble observables but must be related to the physical parameters of the CSPN itself.

The aim of this work is to consider the ISW model in the frame of this so called 'general picture' for the PNe which is described in Sect. 2. Results of the application of the model to NGC 6543 and NGC 6826 are presented in Sect. 3. The conclusions follow in Sect.4.

## 2. PNe: general picture

In order to have a 'general' picture of PNe we have to consider their different parts in a self-consistent manner. This means that the physical parameters (effective temperature, luminosity etc.) of a CSPN must be consistent with its wind characteristics which in turn have to be consistent with the PN parameters (such as nebular radius, expanding velocity etc.). So, in the frame of the general PN picture we make the following basic assumptions:

- the evolution of the CSPN follows according to the standard evolutionary tracks for an AGB-post-AGB star
- the radiation-driven-winds (RDW) theory is applicable to the CSPN wind
- the ISW model is valid

Using these assumptions, the observables of an individual PN have to be analyzed in a self-consistent manner.

### 2.1. Analyses of the CSPN characteristics

The basic CSPN physical parameters are: effective temperature,  $T_{eff}$ , luminosity,  $L$  and radius  $R_*$ . From analyses of the optical and ultraviolet spectra, the least model-dependent parameters: the effective temperature,  $T_{eff}$ , and the ratio  $R_*/d$  (where  $d$  is the distance to the object) can be derived. We remind that the  $T_{eff}$  value is based on the assumed validity of the black-body emission approximation and  $R_*/d$  is derived by making use of

**Table 1.** RDW: adopted force multiplier parameters

	A	B	C
$k$	0.05	0.017	0.085
$\alpha$	0.70	0.740	0.657
$\delta$	0.05	0.115	0.095

some evolutionary track for the CSPN but it does depend only on  $T_{eff}$  and the measured flux (in some spectral range). So, these two quantities are evolutionary track independent. Then to obtain the other parameters we have two choices : a) to adopt an evolutionary track, i.e. to assume a mass for the central star; b) to use the distance usually available only from statistical methods. In the first case we read out  $L$  in the adopted track from the known  $T_{eff}$  and thus derive  $R_*$  and finally  $d$  from the above mentioned ratio. In the second case from the distance  $d$ , we first derive  $R_*$  from the same ratio and next  $L$ . These  $T_{eff}$  and  $L$  will specify an evolutionary track.

Since the mass distribution of observed CSPNs is believed to be quite concentrated around  $0.6 M_{\odot}$ , the assumption of the corresponding evolutionary track (case a) is considered less uncertain than to accept the distance given by the statistical methods (case b).

By assuming as 'typical', in the mentioned sense, the evolutionary track of a  $0.6 M_{\odot}$  star, we have immediately a value for the age of the central star,  $t_{age,CSPN}$ . On the other hand, using the CSPN parameters along the chosen evolutionary track, the CSPN wind characteristics (mass-loss rate, wind velocity) can be derived by making use of the RDW theory. We recall that the mechanical luminosity of the CSPN (fast) wind can be expressed with a power-law function in time within the first few thousands years of the CSPN evolution and this allows a similarity solution for the hot-bubble structure of PNe to be derived (see ZhP for details). This will provide another estimate of age :  $t_{age,ISW}$ . In a self-consistent picture the two ages must be similar and the comparison of them will help to find the best 'general solution' for our object.

We start then considering the most recent evolutionary tracks of a CSPN. They have been calculated for masses in the range between  $0.53$  to  $0.94 M_{\odot}$  (Blöcker, 1995). Our first step has been to derive the 'fast' wind parameters along the tracks for  $0.565$ ,  $0.605$ ,  $0.625 M_{\odot}$  which are nearest to the standard mean mass of CSPNs generally accepted to be very close to  $0.6 M_{\odot}$ . This was done using the RDT theory with the force multiplier parameters  $k, \alpha$  and  $\delta$  (cf. Kudritzki et al., 1992), presented in Table 1 designated as A, B, C. Case A is representative of an O3 star; case B of an O3 star but includes the UV emission from shocks formed in its wind; case C is as B but uses new iron opacities (for details see Kudritzki et al., 1992 and Pauldrach et al., 1994). Clearly there are uncertainties on how the above satisfactory represents real winds particularly in the hottest CSPNs. We have anyhow a representation of fast winds along some significant evolutionary tracks which allows us to apply the ISW theory as formulated in ZhP. The results are shown in Table 2. Note the small differences between the values of  $\beta_1, \beta_2$  and  $\beta$  given by

**Table 2.** CSPN wind parameters

Model	$\Delta t$	$\dot{M}_0 V_0^2$	$\beta_1$	$\dot{M}_0 V_0$	$\beta_2$	$\beta$
(1)	(2)	(3)	(4)	(5)	(6)	(7)
		$M = 0.565 M_\odot$		$lgT_{max} = 5.0$		
A	1000 – 16000	$3.95 \times 10^{-4}$	1.63	$2.90 \times 10^{-6}$	0.52	1.54
B	1000 – 16000	$6.73 \times 10^{-5}$	1.94	$6.08 \times 10^{-7}$	0.76	1.65
C	1000 – 16000	$2.56 \times 10^{-4}$	1.81	$2.57 \times 10^{-6}$	0.69	1.60
		$M = 0.605 M_\odot$		$lgT_{max} = 5.1$		
A	1000 – 6000	$1.74 \times 10^{-3}$	2.28	$7.65 \times 10^{-6}$	0.72	1.76
B	1000 – 6000	$3.71 \times 10^{-4}$	2.67	$1.83 \times 10^{-6}$	1.07	1.89
C	1000 – 6000	$1.46 \times 10^{-3}$	2.49	$8.50 \times 10^{-6}$	0.95	1.83
		$M = 0.625 M_\odot$		$lgT_{max} = 5.2$		
A	300 – 3000	$1.41 \times 10^{-2}$	2.36	$1.80 \times 10^{-5}$	0.80	1.79
B	300 – 3000	$4.29 \times 10^{-3}$	2.70	$5.98 \times 10^{-6}$	1.06	1.90
C	300 – 3000	$1.53 \times 10^{-2}$	2.65	$2.65 \times 10^{-5}$	0.95	1.84

Notes to Table 2:

The RDW models are listed in column (1); column (2) gives the interval of time (in years) for which the corresponding CSPN wind parameters can be fitted by a power-law function. These parameters are given in columns (3)–(7) and the units for columns (3) and (5) are  $M_\odot \text{ yr}^{-1} (\text{ km s}^{-1})^2$  and  $M_\odot \text{ yr}^{-1} \text{ km s}^{-1}$ , respectively. The three different evolutionary tracks are denoted by the CSPN mass and the logarithm of the effective CSPN temperature,  $T_{max}$ , at the upper limit of the considered time interval.

ZhP for the  $0.605 M_\odot$  case and those listed in Table 2. They are due to the use here of newer evolutionary tracks.

## 2.2. Analyses of the PN characteristics

As with the nebula, we consider its radius and expansion velocity. It is well known that the gas velocity may not be uniform through the nebula and this is why the expansion velocity of a given PN might have a bit different values if optical lines of various ions are used. Unfortunately, our 1D model does not allow to treat this item in detail and the value of the expansion velocity is attributed to the gas near the outer radius of the optical shell. The latter radius is assumed to be the radius of the PN. Thus, from the ZhP model we have that the radius of the PN can be expressed through the fast and the slow wind parameters:

$$R_2 = \left[ \frac{1}{\beta(2\beta - 1)(5\beta - 2)} \frac{\dot{M}_0 V_0^2}{\dot{M}_{sw} V_{sw}^2} \right]^{1/3} (V_{sw} t_0) \tau^\beta \quad (1)$$

where  $\dot{M}_{fw} V_{fw}^2 = \dot{M}_0 V_0^2 \tau^{\beta_1}$ ,  $\tau = \frac{t}{t_0}$ ,  $t_0 = 1000 \text{ yr}$ ,  $\beta = \frac{\beta_1}{3} + 1$  and  $\dot{M}_{fw} V_{fw} = \dot{M}_0 V_0 \tau^{\beta_2}$  (see Table 2 for the values of corresponding parameters). And from here one gets that

$$t_{age,ISW} = \beta \frac{R_2}{V_{exp}} = \beta t_{exp} \quad (2)$$

where  $V_{exp}$  is the observed PN expansion velocity and  $t_{age,ISW}$  is the corresponding nebular age according to the ISW model.

Thus having from observations the expansion velocity and the radius of a PN, we can check whether the nebula age,  $t_{age,ISW}$ , is consistent with the CSPN age,  $t_{age,CSPN}$ , as derived from an evolutionary track. We note that in the frame of the ISW model the 'traditional' expansion age,  $t_{exp}$ , is not equal to the true nebular age since the CSPN wind parameters are function of time.

Finally, from the consistency of the mentioned stellar and nebular ages, one can estimate the slow wind parameters  $\frac{\dot{M}_{sw}}{V_{sw}}$  which then allows quantitative predictions for the hot-bubble characteristics to be made. In fact, in the frame of the ISW model, once having the age of the PN, formulae (1) and (2) can be used to have two independent estimates of the slow wind parameter  $\frac{\dot{M}_{sw}}{V_{sw}}$  if the PN expansion velocity and the radius are known. Then, having calculated further observables of a given PN (X-ray, EUV and IRCL characteristics), they can be confronted with those observed and thus further constraints can be placed on the ISW model. Of course, the applicability of the general PNe picture is limited by the uncertainties of the object parameters due both to observations and theories applied. As a first attempt we apply the proposed scheme to two PNe which have relatively well known parameters.

## 3. Results and discussion

We apply the above described 'general picture' of PNe to NGC 6543 and NGC 6826. For each object we first use method (a), then method (b) to derive the needed star and nebular parameters. We then analyze the nebular radius and expansion velocity in the frame of the ISW model (&2.2). We compare the resulting nebular age with that associated to the central star coming from the relevant evolutionary track. We also calculate the expected radiation from the hot nebular bubble in the two objects and compare with the observed X-ray radiation.

### 3.1. NGC 6543

Extended X-ray radiation has been definitely observed in this PN, according to Kreysing et al. (1992). This is important for our 'general picture' of a PN, which should make use of as many observables as possible. We then tentatively apply our model to this object, in spite of the difficulties with the complex

morphology of its inner fine structures (Balick et al., 1997) and with the central star having WR characteristics. We would like to warn that there may be difficulties when applying the RDW theory to a CSPN with WR spectral characteristics. Also, the use of the standard AGB-post-AGB evolutionary tracks in such a case is not much justified considering the unclear evolutionary status of such CSPNs. On the other hand, this is at present the only possibility to carry out an analysis in the frame of the general PNe picture. Thus, we consider our analysis of NGC 6543 as a zeroth approach to the problem.

To derive the stellar and nebular parameters, we first apply method (a). A good set of parameters for the central star of NGC 6543 is likely :  $T_{eff} = 60000 \pm 10000K$ ;  $\lg(L/L_{\odot}) = 3.75$ ;  $R_*/R_{\odot} = 0.7$ ;  $R_*/d = 1.1 \times 10^{-11}$ ;  $d = 1.44$  kpc;  $\dot{M}_{fw} = 4 \times 10^{-8} M_{\odot} \text{ yr}^{-1}$ ;  $V_{fw} = 1900 \text{ km s}^{-1}$  (Perinotto et al., 1989). We recall that the effective temperature,  $T_{eff}$ , the ratio of the stellar radius to the distance to the object,  $R_*/d$ , and  $V_{fw}$  are relatively well determined while the other quantities follow from the assumed typical evolutionary track of a post-AGB model of  $M = 0.6 M_{\odot}$  (cf. Perinotto et al., 1989). The recent evolutionary track of a CSPN having stellar mass  $M = 0.605 M_{\odot}$  (Blöcker, 1995) would give, combined with the above  $T_{eff}$ , the luminosity :  $\lg(L/L_{\odot}) = 3.78$  and then a set of parameters essentially identical to the above ones. The evolutionary stellar age  $t_{age,CSPN}$  corresponding to this recent track is of about 3500 years while the measured  $V_{fw}$  is consistent with a stellar age of about 4000 years if the RDW theory is applied to this  $0.605 M_{\odot}$  mass track.

We search now the nebular age. In NGC 6543 we accept for the expansion velocity and the nebular radius :  $V_{exp} = 20 \text{ km s}^{-1}$  (Weinberger, 1989) and  $R_2 = 0.056$  pc, where the latter value has been scaled from the one given by Weinberger (1989), to be consistent with the distance of 1.44 kpc. From Eq. (2) we then derive  $t_{age,ISW} = 5100$  years, relatively close to the above  $t_{age,CSPN} = 3500$  years, from the stellar evolutionary track.

We apply now method (b). The mean distance from various determinations with statistical methods, excluding just the largest and the smallest one (see Acker et al., 1992), amounts to  $d = 1$  kpc. Using  $T_{eff}$  and  $R_*/d$  as above, we have the following values for the other stellar parameters :  $R_*/R_{\odot} = 0.49$ ;  $\lg(L/L_{\odot}) = 3.46$  and  $\dot{M}_{fw} = 2.8 \times 10^{-8} M_{\odot} \text{ yr}^{-1}$  ( $V_{fw}$  does not change since it does not depend on the distance). The above  $T_{eff}$  and the new  $\lg(L/L_{\odot})$  call for an evolutionary track with a mass smaller than  $0.605 M_{\odot}$ . The next available track from Blöcker (1995) is for  $0.565 M_{\odot}$ . This track implies  $t_{age,CSPN} = 11000$  years.

On the other hand the nebular radius corresponding to the distance of 1 kpc is  $R_2 = 0.039$  pc. This provides  $t_{age,ISW} = 3600$  years. Now the separation of the two ages is quite larger than before.

We consider this as an argument that method (b) works in this object less well than method (a). Probably method (a) applied to an evolutionary track a bit more luminous than that of  $0.605 M_{\odot}$ , i.e. to a star a bit more massive would provide a still better solution. But in view of the uncertainties, we consider

appropriate at present to accept the above discussed solution obtained with method (a).

Since we would like to have additional constraints on the PN physics, we have modelled the X-ray, EUV and IRCL emission of NGC 6543. In order to have an idea about the effect of the distance uncertainties on the hot-bubble emission we have done two sets of models related with two values for the distance to the object: 1.0 and 1.44 kpc. The corresponding models are numbered 1,2,3 (PN age of 3500, 4000 and 4500 years); 4,5,6 (PN age of 3500, 4000 and 4500 years) for the two distances, respectively. Additionally, we have considered the three different sets of the RDW model parameters (see Table 1). The results are presented in Fig. 1 and Table 3. Columns 3 and 4 in Table 3 show the internal consistency of the procedure (+ and – signs mean whether the model value is bigger or smaller than that deduced from observations). We see that the nebular PN parameters, its radius and expansion velocity, are acceptably well reproduced in the frame of the ISW model along a  $0.605 M_{\odot}$  mass evolutionary track and applying the RDW theory with different force multiplier parameters. Also, column 2 in Table 3 gives the mean value of the slow wind quantity  $\frac{\dot{M}_{sw}}{V_{sw}}$  derived from the 'observed'  $R_2$  and  $V_{exp}$ . If we assume a slow wind velocity of about  $10 \text{ km s}^{-1}$  then it is derived that  $\dot{M}_{sw} = (afew) \times 10^{-6} \div 10^{-5} M_{\odot} \text{ yr}^{-1}$ , a value which can be considered typical for an AGB star. We mention that this value is at least one order of magnitude smaller than that expected for the 'superwind' of about  $10^{-4} M_{\odot} \text{ yr}^{-1}$ .

Fig. 1 shows the theoretical X-ray spectra of NGC 6543. It can be seen that the shape of the X-ray spectrum is not sensitive to the model parameters while Models A and C give about 4–5 times higher fluxes and 'net' luminosities (see also columns 5 and 6 in Table 3). Given the values in Table 2, this result can be well understood in terms of the higher mass-loss rates of the CSPN wind as derived in Models A and C with respect to Model B. A higher mass loss rate suggests a higher mass of the hot bubble since the gas evaporation from the cold shell (optical PN) will be more efficient in this case. A comparison between the spectra in Fig. 1 and those in Fig. 3 of Kreysing et al. (1992) shows that the model predictions based on the ISM theory correspond fairly well to the observed X-ray characteristics of NGC 6543. Namely, the calculated and observed spectra are similar not only qualitatively, having similar shape and 'softness', but they show a quantitative correspondence as well (see the y-axes in the cited figures which give the flux density). On the other hand, X-ray observations with better spatial resolution are highly desirable because if the X-ray emission has a larger extension than the optical one (as claimed by Kreysing et al., 1992), then a more complex physics would be required to explain the X-ray properties.

Since the results presented here are based on the CSPN parameters (mass loss rate and wind velocity) predicted by the radiation-driven-wind theory (Pauldrach et al., 1988) another item is also of some interest. Namely, the results presented in Table 2 allow to estimate that for  $t_{age,CSPN} = 3500 - 4500$  years the CSPN wind velocity is:  $V_{fw} = 1600 \div 2400 \text{ km s}^{-1}$

**Table 3.** NGC 6543: results

No.	$\frac{\dot{M}_6}{V_{10}}$ mean	$R_2$ (%)	$V_{exp}$ (%)	$L_X$ 0.05–2.5 keV	$F_X$ 0.05–2.5 keV	$L_{EUV}$ 70–700 Å	$L_{NeV}$ 24.3 μ	$L_{NeVI}$ 7.65 μ	$L_{SiIX}$ 3.92 μ	$L_{FeX}$ 6374 Å
(1)	(2)	(3)	(4)	(5)	(6)	(7)	(8)	(9)	(10)	(11)
A1	5.8	+2.0	-2.0	$1.3 \times 10^{33}$	$3.0 \times 10^{-13}$	$4.2 \times 10^{33}$	$1.7 \times 10^{29}$	$1.8 \times 10^{29}$	$6.1 \times 10^{28}$	$1.1 \times 10^{29}$
A2	9.9	+7.8	-9.3	$1.9 \times 10^{33}$	$5.3 \times 10^{-13}$	$6.2 \times 10^{33}$	$2.4 \times 10^{29}$	$2.6 \times 10^{29}$	$9.5 \times 10^{28}$	$1.7 \times 10^{29}$
A3	16.5	+12.1	-16.1	$2.9 \times 10^{33}$	$9.1 \times 10^{-13}$	$9.2 \times 10^{33}$	$3.5 \times 10^{29}$	$3.8 \times 10^{29}$	$1.5 \times 10^{29}$	$2.5 \times 10^{29}$
A4	3.8	-18.3	+13.3	$1.7 \times 10^{33}$	$1.8 \times 10^{-13}$	$5.8 \times 10^{33}$	$2.3 \times 10^{29}$	$2.5 \times 10^{29}$	$8.1 \times 10^{28}$	$1.5 \times 10^{29}$
A5	5.8	-10.4	+8.6	$2.1 \times 10^{33}$	$2.6 \times 10^{-13}$	$7.1 \times 10^{33}$	$2.8 \times 10^{29}$	$3.0 \times 10^{29}$	$1.0 \times 10^{29}$	$1.8 \times 10^{29}$
A6	8.7	-3.9	+3.6	$2.8 \times 10^{33}$	$3.7 \times 10^{-13}$	$8.9 \times 10^{33}$	$3.4 \times 10^{29}$	$3.7 \times 10^{29}$	$1.4 \times 10^{29}$	$2.4 \times 10^{29}$
B1	2.2	-1.6	+1.6	$3.0 \times 10^{32}$	$3.8 \times 10^{-14}$	$1.2 \times 10^{33}$	$5.1 \times 10^{28}$	$5.3 \times 10^{28}$	$1.2 \times 10^{28}$	$2.4 \times 10^{28}$
B2	4.0	+4.8	-5.3	$4.8 \times 10^{32}$	$7.4 \times 10^{-14}$	$1.8 \times 10^{33}$	$7.5 \times 10^{28}$	$8.0 \times 10^{28}$	$2.1 \times 10^{28}$	$4.0 \times 10^{28}$
B3	6.8	+9.6	-11.9	$7.7 \times 10^{32}$	$1.4 \times 10^{-13}$	$2.8 \times 10^{33}$	$1.1 \times 10^{29}$	$1.2 \times 10^{29}$	$3.5 \times 10^{28}$	$6.6 \times 10^{28}$
B4	1.5	-22.5	+15.4	$4.4 \times 10^{32}$	$2.5 \times 10^{-14}$	$1.8 \times 10^{33}$	$7.8 \times 10^{28}$	$8.1 \times 10^{28}$	$1.7 \times 10^{28}$	$3.5 \times 10^{28}$
B5	2.4	-14.5	+11.3	$5.8 \times 10^{32}$	$3.9 \times 10^{-14}$	$2.3 \times 10^{33}$	$9.6 \times 10^{28}$	$1.0 \times 10^{29}$	$2.4 \times 10^{28}$	$4.8 \times 10^{28}$
B6	3.8	-7.8	+6.8	$7.9 \times 10^{32}$	$6.2 \times 10^{-14}$	$3.0 \times 10^{33}$	$1.2 \times 10^{29}$	$1.3 \times 10^{29}$	$3.5 \times 10^{28}$	$6.7 \times 10^{28}$
C1	6.7	0.0	0.0	$1.6 \times 10^{33}$	$4.0 \times 10^{-13}$	$5.2 \times 10^{33}$	$2.1 \times 10^{29}$	$2.2 \times 10^{29}$	$7.8 \times 10^{28}$	$1.4 \times 10^{29}$
C2	11.7	+6.2	-7.1	$2.5 \times 10^{33}$	$7.3 \times 10^{-13}$	$7.9 \times 10^{33}$	$3.0 \times 10^{29}$	$3.3 \times 10^{29}$	$1.2 \times 10^{29}$	$2.1 \times 10^{29}$
C3	19.6	+10.8	-13.8	$3.9 \times 10^{33}$	$1.3 \times 10^{-12}$	$1.2 \times 10^{34}$	$4.4 \times 10^{29}$	$4.8 \times 10^{29}$	$1.9 \times 10^{29}$	$3.3 \times 10^{29}$
C4	4.5	-20.6	+14.5	$2.3 \times 10^{33}$	$2.6 \times 10^{-13}$	$7.6 \times 10^{33}$	$3.0 \times 10^{29}$	$3.2 \times 10^{29}$	$1.1 \times 10^{29}$	$2.0 \times 10^{29}$
C5	7.0	-12.7	+10.1	$2.9 \times 10^{33}$	$3.8 \times 10^{-13}$	$9.4 \times 10^{33}$	$3.7 \times 10^{29}$	$4.0 \times 10^{29}$	$1.4 \times 10^{29}$	$2.5 \times 10^{29}$
C6	10.8	-6.0	+5.4	$3.9 \times 10^{33}$	$5.6 \times 10^{-13}$	$1.2 \times 10^{34}$	$4.6 \times 10^{29}$	$5.0 \times 10^{29}$	$1.9 \times 10^{29}$	$3.3 \times 10^{29}$

Notes to Table 3:

column (1): the model number; column (2): the slow wind parameter  $\frac{\dot{M}_{sw}}{V_{sw}}$  where  $\dot{M}_{sw}$  is in units of  $10^{-6} M_{\odot} \text{ yr}^{-1}$  and  $V_{sw}$  is in units of  $10 \text{ km s}^{-1}$ ; columns (3) and (4): the deviation (in per cent) between the theoretically and observationally derived values of the PN radius and expansion velocity; columns (5) ÷ (11): the X-ray, EUV and IRCL luminosities (of certain lines) in units of  $\text{erg s}^{-1}$

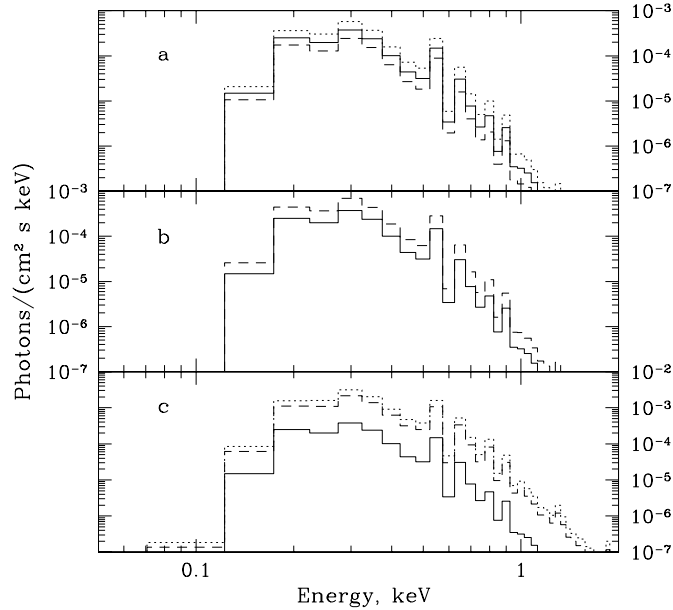


**Fig. 1a–c.** The theoretical X-ray spectrum of NGC 6543 attenuated by the absorption of the interstellar medium having  $N_H = 7.2 \times 10^{20} \text{ cm}^{-2}$ , a value corresponding to a reddening of  $E_{B-V} = 0.12$ . **a** spectra for models B4 (dashed line), B5 (solid line) and B6 (dots); **b** spectra for models B2 (dashed line), B5 (solid line); **c** spectra for models A5 (dashed line), B5 (solid line) and C5 (dots), see Table 3.

(Model A);  $V_{fw} = 1500 \div 2200 \text{ km s}^{-1}$  (Model B)  $V_{fw} = 1200 \div 1750 \text{ km s}^{-1}$  (Model C) and the corresponding val-

ues for the CSPN mass loss are:  $\dot{M}_{fw} = 1 \times 10^{-8} M_{\odot} \text{ yr}^{-1}$  (Model A);  $\dot{M}_{fw} = 4.3 \times 10^{-9} M_{\odot} \text{ yr}^{-1}$  (Model B);  $\dot{M}_{fw} = 2 \times 10^{-8} M_{\odot} \text{ yr}^{-1}$  (Model C). A comparison with the values of these quantities deduced from observations (see above) shows that the model predicted wind velocity value corresponds well to that observed especially for Models A and B (for Model C this is true only for a PN age of 4000–4500 years). On the other hand, the theoretical mass-loss rate, predicted by Model B, is an order of magnitude smaller than the ‘observed’ one while Models A and C (particularly Model C) show an acceptable correspondence with observations. This analysis definitely demonstrates that well defined force multipliers parameters are needed for the case of the CSPN winds. Further work in this direction is strongly desired.

We conclude that the X-rays data appear to confirm the general PN picture of NGC 6543 given above with a distance close to 1.4 kpc.

### 3.2. NGC 6826

NGC 6826 is another object with relatively well known parameters. Its rather regular shape suggests that applying a 1-D model would be quite suitable in this case.

We start applying method (a) to derive the basic parameters. A set of parameters for the CSPN in NGC 6826 is:  $T_{eff} = 45000 \pm 10000 \text{ K}$ ;  $\lg(L/L_{\odot}) = 3.88$ ;  $R_*/R_{\odot} = 1.45$ ;  $R_*/d = 1.09 \times 10^{-11}$ ;  $d = 2.99 \text{ kpc}$ ;  $\dot{M}_{fw} = 5.2 \times 10^{-8} M_{\odot} \text{ yr}^{-1}$ ;  $V_{fw} = 1750 \text{ km s}^{-1}$ . (Perinotto et al., 1989). They have been

derived with the same procedure as the corresponding ones of NGC 6543. The recent evolutionary track of a CSPN having stellar mass  $M = 0.605 M_{\odot}$  would indicate, combined with the above  $T_{eff}$ , an evolutionary stellar age of  $t_{age,CSPN}$  of about 3000–4000 years and  $\lg(L/L_{\odot}) = 3.79$  which will result in a corresponding change of the other CSPN parameters, i.e.:  $R_{*}/R_{\odot} = 1.31$ ,  $d = 2.7$  kpc and  $\dot{M}_{fw} = 4.7 \times 10^{-8} M_{\odot} \text{ yr}^{-1}$ . The measured  $V_{fw}$  is consistent with a stellar age of about 3800 years if the RDW theory is applied to the case of a  $0.605 M_{\odot}$  mass star.

We adopt for NGC 6826 the nebular parameters:  $V_{exp} = 27 \text{ km s}^{-1}$ ,  $R_2 = 0.061 \text{ pc}$  at  $d = 1 \text{ kpc}$  (Weinberger, 1989). By scaling from the distance  $d = 1 \text{ kpc}$ , used by Weinberger, to  $d = 2.7 \text{ kpc}$ , the radius becomes  $R_2 = 0.165 \text{ pc}$ . Eq. (2) then gives  $t_{age,ISW} = 11200$  years. We see that using method (a) we end up with quite different ages for the CSPN and the nebula in NGC 6826.

We then follow method (b) assuming as valid for NGC 6826 the distance based on various statistical determinations. Looking at Acker et al. (1992), we see that eighth different measurements concentrate around  $d = 1 \text{ kpc}$ . Thus, the nebular NGC 6826 parameters:  $V_{exp} = 27 \text{ km s}^{-1}$ ,  $R_2 = 0.061 \text{ pc}$  at  $d = 1 \text{ kpc}$  (Weinberger, 1989) suggest  $t_{age,ISW} = 4150$  years. On the other hand, the measured  $T_{eff}$  and  $R_{*}/d$  imply at this distance of  $1 \text{ kpc}$ ,  $R_{*}/R_{\odot} = 0.54$ ;  $\lg(L/L_{\odot}) = 2.93$  and  $\dot{M}_{fw} = 1.9 \times 10^{-8} M_{\odot} \text{ yr}^{-1}$ . It is worth noting that these values of  $T_{eff}$  and  $L$  demand for this object an evolutionary track quite different from the standard one, i. e. with a quite smaller mass.

In the grid of models calculated by Blöcker (1995), the one for  $M = 0.546 M_{\odot}$  would appear to have the proper luminosity, close to  $\lg(L/L_{\odot}) = 2.93$ . The age corresponding to the observed  $T_{eff} = 45000 \text{ K}$  would be however very much larger than any plausible value derived from the observed nebular  $V_{exp}$  and the nebular radius. The track relative to  $0.565 M_{\odot}$  is, from this point of view, quite more acceptable.

With this evolutionary track of  $0.565 M_{\odot}$ , the observed  $T_{eff}$  implies an age of about 8 000 years. The luminosity would be  $\lg(L/L_{\odot}) = 3.58$  which in turn suggests  $R_{*}/R_{\odot} = 1.03$ ; and from the observed  $R_{*}/d$  a value of  $2.12 \text{ kpc}$  for the distance to the object comes out. The mass loss rate of the fast wind would now be  $\dot{M}_{fw} = 3.7 \times 10^{-8} M_{\odot} \text{ yr}^{-1}$ .

For the distance of  $2.12 \text{ kpc}$ , the PN radius becomes  $0.129 \text{ pc}$ . The PN age derived from the ISW model, if again a value of  $27 \text{ km s}^{-1}$  is assumed for the PN expansion velocity, is of  $7 500$  years, very close to the above value of  $8 000$  years.

In order to have more constraints on the physics of the PN system in NGC 6826 we will further proceed by considering some direct observables of the hot bubble (being a cornerstone for the ISW model). As in the case of NGC 6543, we have modelled the X-ray, EUV and IRCL emission of NGC 6826 for the three different sets of the RDW force multipliers parameters given in Table 1. The results are presented in Fig. 2 and Table 4. As seen from columns 3 and 4 of Table 4, the nebular PN parameters are acceptably well reproduced in the frame of the ISW model along the  $0.565 M_{\odot}$  mass evolutionary track and applying the RDW theory with different force multiplier pa-

rameters. Also, column 2 in the same table gives that the slow wind characteristic  $\frac{\dot{M}_{sw}}{V_{sw}}$  derived from the 'observed'  $R_2$  and  $V_{exp}$  suggests that  $\dot{M}_{sw} = 0.2 \div 0.8 \times 10^{-6} M_{\odot} \text{ yr}^{-1}$ , if we again assume a slow wind velocity of about  $10 \text{ km s}^{-1}$ . It is worth noting that as in the case of NGC 6543 this value is one–two orders of magnitude smaller than that usually quoted for the 'superwind'.

The theoretical X-ray spectrum can be seen in Fig. 2 and from there and Table 4 it is immediate that while the 'net' X-ray luminosity is about an order of magnitude smaller than that for NGC 6543 the X-ray flux is about 1.5–2 orders of magnitude less. Moreover the X-ray spectrum is expected to be softer than in the previous case. This results from the smaller interstellar extinction ( $E_{B-V} = 0.02$  vs.  $E_{B-V} = 0.12$ ).

The above is consistent with the fact that an observed X ray flux from NGC 6826 has not been reported. NGC 6826 is in fact neither listed among the PNe detected nor among those observed but not detected by ROSAT (Conway & Chu, 1997). A further effort (Conway, priv. communications) shows that it does not belong presently to the Pointed Observations Catalogue, neither is listed in the ROSAT Bright Star Catalogue. The latter information, considering that it is extremely unlikely it falls in the few locations missed from the ROSAT all sky survey, allows to put for NGC 6826 an upper limit of  $0.05 \text{ cts/s}$ , a value a few times larger than the observed flux from NGC 6543 (Kreysing et al., 1992). This limit is however too high to offer some useful constraint with respect to our predicted X-ray flux in NGC 6826. On the other hand the above information from the ROSAT satellite, taken together, is consistent with a flux from this source quite below that from NGC 6543, and then in agreement with our predictions.

In any case a comparison between Fig. 2a and Fig. 2b gives an idea about the differences in the theoretical X-ray characteristics of NGC 6826 between the  $0.565 M_{\odot}$  and  $0.605 M_{\odot}$  mass cases. A corresponding difference in the EUV and IRCL luminosities is evidently found.

Using the results from Table 2, we have the model predicted CSPN wind velocity,  $1000\text{--}1400 \text{ km s}^{-1}$  (the lower limit is for Model C) which is a bit lower than the value deduced from observations and the theoretical CSPN mass loss is  $\dot{M}_{fw} = 2.2 \times 10^{-9} \div 1.0 \times 10^{-8} M_{\odot} \text{ yr}^{-1}$  (the lower limit is for Model B). This confirms the previously drawn conclusion about the importance of the correct RDW modelling of the CSPN winds.

Thus, future observations of X-rays in NGC 6826 would be especially important to possibly confirm the general picture of this object we have offered.

#### 4. Conclusions

We have made an attempt to present a so called general picture for PNe which is based on the assumption that the PN and CSPN characteristics must be understood in the global frame of the theories applied in this case. These theories are: (i) the RDW model; (ii) the theory for evolution of an AGB-post-AGB star; (iii) the ISW wind for PNe. We used in our study the one-dimensional two-winds model of Zhekov & Perinotto (1996)

**Table 4.** NGC 6826: results

No.	$\frac{\dot{M}_6}{V_{10}}$ mean	$R_2$ (%)	$V_{exp}$ (%)	$L_X$ 0.05–2.5 keV (5)	$F_X$ 0.05–2.5 keV (6)	$L_{EUV}$ 70–700 Å (7)	$L_{NeV}$ 24.3 μ (8)	$L_{NeVI}$ 7.65 μ (9)	$L_{SiIX}$ 3.92 μ (10)	$L_{FeX}$ 6374 Å (11)
A	0.7	+4.7	-5.1	$5.7 \times 10^{31}$	$5.6 \times 10^{-15}$	$3.0 \times 10^{32}$	$1.4 \times 10^{28}$	$1.3 \times 10^{28}$	$1.3 \times 10^{27}$	$3.3 \times 10^{27}$
B	0.2	+1.6	-1.7	$1.1 \times 10^{31}$	$5.5 \times 10^{-16}$	$7.1 \times 10^{31}$	$3.4 \times 10^{27}$	$2.9 \times 10^{27}$	$8.5 \times 10^{25}$	$3.0 \times 10^{26}$
C	0.7	+2.9	-3.1	$5.7 \times 10^{31}$	$5.4 \times 10^{-15}$	$3.0 \times 10^{32}$	$1.4 \times 10^{28}$	$1.3 \times 10^{28}$	$1.3 \times 10^{27}$	$3.2 \times 10^{27}$

Notes to Table 4:

column (1): the model number; column (2): the slow wind parameter  $\frac{\dot{M}_{sw}}{V_{sw}}$  where  $\dot{M}_{sw}$  is in units of  $10^{-6} M_{\odot} \text{ yr}^{-1}$  and  $V_{sw}$  is in units of  $10 \text{ km s}^{-1}$ ; columns (3) and (4): the deviation (in per cent) between the theoretically and observationally derived values of the PN radius and expansion velocity; columns (5) ÷ (11): the X-ray, EUV and IRCL luminosities (of certain lines) in units of  $\text{erg s}^{-1}$

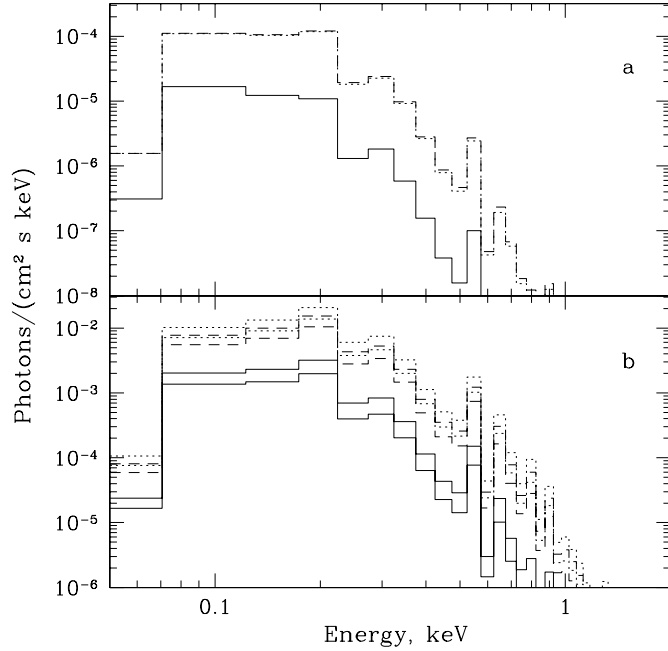


**Fig. 2a and b.** The theoretical X-ray spectrum of NGC 6826 attenuated by the absorption of the interstellar medium having  $N_H = 1.2 \times 10^{20} \text{ cm}^{-2}$ , a value corresponding to a reddening of  $E_{B-V} = 0.02$ . —bf a spectra in the case of  $0.565 M_{\odot}$  mass CSPN at a PN age of 8 000 years; the dashed, solid and dotted lines present the results of Models A, B and C, respectively, see Table 4. **b** spectra in the case of  $0.605 M_{\odot}$  mass CSPN; the dashed, solid and dotted lines present the results of Models A, B and C, respectively, and for  $t_{age, ISW} = 3500$  and 4000 years.

applied to two PNe (NGC 6543 and NGC 6826) and the main results can be summarized as follow:

- NGC 6543: The CSPN age (according to the  $0.605 M_{\odot}$  mass track) and the age of the nebula are consistent (given by the ISW mode) with a value of about 4000 years. The model predicted (ISW model) X-ray characteristics of this object are in accordance with those deduced from observations. The general PNe picture gives preference to a distance value of 1.4 kpc.
- NGC 6826: A self-consistent general picture of PNe is possible along the evolutionary track of  $0.565 M_{\odot}$  mass for the

CSPN in NGC 6826. As a result a value close to 2 kpc looks appropriate for the distance to this object. Future X-ray observations are of great importance for proper confrontation with predictions from the theory in this case.

- For both objects, the general PNe picture suggests that the so-called super-wind had a mass loss of 1–2 orders of magnitude smaller than the traditionally accepted value of  $10^{-4} M_{\odot} \text{ yr}^{-1}$ .
- The force multiplier parameters (from the RDW model) play important role for the general picture of PNe. A development of the RDW theory towards higher photospheric temperature is highly desired.

*Acknowledgements.* The authors thank Dr.T.Blöcker for providing detailed data on his recent evolutionary tracks for CSPN. The authors are grateful to the referee Dr.G.Mellema for criticism and valuable suggestions. SZh acknowledges the Visiting Professor programme of GNA-CNR at Osservatorio Astrofisico di Arcetri, Firenze, Italy where part of this work has been done. This work was also partially sponsored by the National Science Fund of the Bulgarian Ministry of Education, Science and Technologies under contract F-570.

## References

- Acker A., Ochsenbein F., Stenholm B. et al., 1992, 'Strasbourg – ESO Catalogue of Galactic Planetary Nebulae', ESO
- Arnaud K., Borkowski K. J., Harrington J. P., 1996, ApJL 462, L75
- Balick B., Alexander J., Hajian A. et al., 1997, in IAU Symp. 180, Planetary Nebulae, eds. H. J. Habing, H. J. G. L. M. Lamers, Kluwer, Dordrecht, in press.
- Blöcker T., 1995, A&A 299, 755
- Conway G. M., You-Hua Chu, 1997, in IAU Symp., No.180, Planetary Nebulae, eds. H. J. Habing, H. J. G. L. M. Lamers, Kluwer, Dordrecht, in press.
- Greenhouse M. A., Feldman U., Smith H. A. et al., 1993, ApJS 88, 23
- Kahn F. D., 1983, in IAU Symp., No.103, Planetary Nebulae, ed. D. R. Flower, Kluwer, Dordrecht, 305
- Kreysing H. C., Diesch C., Zweigle J. et al., 1992, A&A 264, 623
- Kudritzki R.P., Hummer D.G., Pauldrach A. et al., 1992, A&A 257, 655
- Kwok S., 1983, in IAU Symp., No.103, Planetary Nebulae, ed. D. R. Flower, Kluwer, Dordrecht, 293
- Kwok S., Purton C. R., Fitzgerald P. M., 1978, ApJL 219, L125
- Mellema G., Frank A., 1995, MNRAS 273, 401
- Patriarchi P., Perinotto M., 1991, A&AS 91, 325

- Pauldrach A.W.A., Kudritzki R.P., Puls J., Butler K., Hunsinger, J., 1994, A&A 283, 525
- Pauldrach A., Puls J., Kudritzki R. P., Mendez R. H., Heap S. R., 1988, A&A 207, 123
- Perinotto M., 1993, in IAU Symp. No.155, Planetary Nebulae, eds. R. Weinberger and A. Acker, Kluwer, Dordrecht, 57
- Perinotto M., Cerruti-Sola M., Lamers H. J. G. M. L., 1989, ApJ 337, 283
- Soker N., 1994, AJ 107, 276
- Weinberger R., 1989, A&AS 78, 301
- Zhekov S. A., Perinotto M., 1996, A&A 309, 648